

Origin of Gamma-Ray Bursts Progenitor and Iron line diagnosis

Toshio MURAKAMI*

*Institute of Space and Astronautical Science, 3-1-1, Yoshinodai, Sagami-hara, Kanagawa 229-8510
murakami@astro.isas.ac.jp*

A possibility of particle accelerations to UHE/EHE in Gamma-Ray Burst (GRBs) is discussed in separate papers in this volume, so I focus on the origin of GRBs, especially a progenitor of GRB in view point of the observed iron diagnosis. Iron spectral features are thought to be the best tracer of a progenitor of GRBs. The detections of spectral features such as an iron emission line and/or a Radiative Recombination edge and Continuum (RRC) were reported in a few afterglows of GRBs. However their properties are different each other. For example, Chandra observation of GRB 991216 reported the strong H-like iron line together with its RRC feature. On the contrary, ASCA reported only a detection of the strong RRC feature in GRB 970828. Since it is difficult to produce the strong RRC, we have to consider some special condition for the line and/or the RRC forming region. In this paper, we point out a possibility of a “*non-equilibrium ionization state*” for the line and the RRC forming region. The existence of the RRC iron features strongly suggests a dense circumstellar matter surrounding a progenitor, which might be produced at the time of a supergiant phase of a massive star

KEYWORDS: gamma-ray bursts, iron line, progenitor

§1. Introduction

Gamma-Ray Bursts (GRBs) are now established to be remote at cosmological distances and thus their released energies in γ -ray photons are almost $\sim 10^{52}$ erg.¹⁾ This is the largest energy release in the universe in photons. Although fireball models^{2,3)} or a cannonball model⁴⁾ can explain many observational properties of GRBs, especially the power-law decay in flux, bright optical transients and the time evolution of them, however a progenitor of GRB, which is suspected to be a black-hole, is yet to be solved. The best review paper of the most recent afterglow observations and the theoretical works related to the fireball is in the Annual Review of Astronomy and Astrophysics volume 35, 2000 by J. v. Paradijs, C. Kouveliotou and R. M. J. Wijers⁵⁾ and a possibility to accelerate particles to EHE in GRBs is widely discussed in this volume. So I focus on just the iron line physics related to a progenitor of GRBs.

I think that an important key to probe a progenitor of a GRB is the detection of iron spectral features in X-ray afterglows, however the details of the recent observations were not discussed in their review by Paradijs et al.⁵⁾ Iron is the most abundant heavy element and fall in the middle of the observed energy range of the X-ray satellites such as ASCA, BeppoSAX and Chandra. Not to say, the strong iron spectral features can be produced in a dense gas environment of a massive progenitor. Therefore, the iron detections support the best evidence of a collapsing model of a massive star such as Hypernova/Collapsar or Supranova⁶⁻⁸⁾ and reject the

binary merger type models.

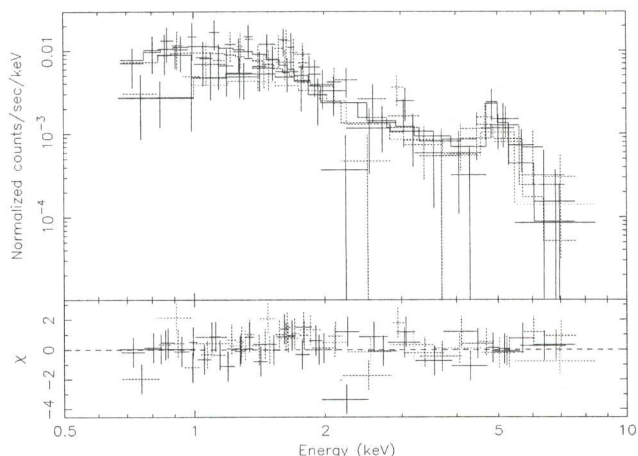


Fig. 1. The observed X-ray spectrum. The first detection of the iron spectral feature at ~ 5 keV with ASCA. The line looks somewhat broaden and measures the redshift to be ~ 0.33 assuming a He-like iron. Later, this feature is interpreted as the result of the Radiative Recombination edge and Continuum (RRC) at $z = 0.9578$

§2. Iron Detections

The iron features were already reported in four X-ray afterglows. The early two reports are as follows. The redshifted iron emission line was discovered in the X-ray afterglow of GRB 970508 with BeppoSAX,⁹⁾ and the redshift was consistent with the distance of a host galaxy.

* Also: Department of Physics, Tokyo Institute of Technology, 2-12-1 Ookayama, Meguro, Tokyo 152-0033, Japan

An independent discovery of a redshifted iron emission line was reported for GRB 970828 with ASCA.^{10,20)} Assuming a He-like $K\alpha$ line, the spectral feature was once interpreted as an emission line with a redshift of $z = 0.33$. However, the Keck observation of the host galaxy, which was discovered later in 1998, revealed the redshift of $z = 0.9578$.¹¹⁾ The discrepancy in distance with ASCA and the temporal detections shown in fig. 2 of the iron feature with ASCA and BeppoSAX forced us to doubt the reality of existence of the iron features before the confirmation by the Chandra detection.

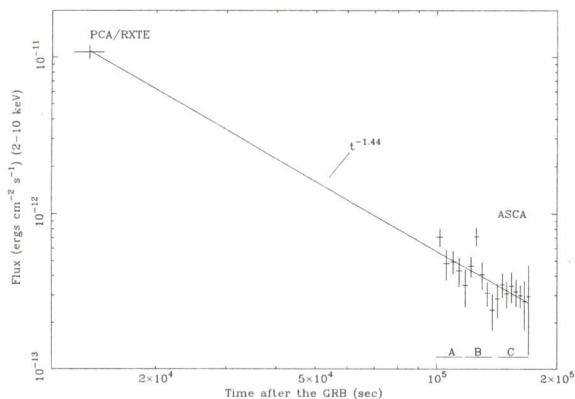


Fig. 2. The iron detection was temporal. The X-ray light curve obtained with ASCA is plotted together with the flux reported by Marshall et al (1997). Here we assume a power-law spectrum with the photon index of -2 for the flux calculation. The simple power-law decay model is indicated by the solid line: $t^{-1.44 \pm 0.07}$. The lines labeled “A”, “B” and “C” indicate the intervals for which spectral studies are made. The line appeared only during the interval B.

In 1999, Chandra observed GRB 991216 at 37 hours after the GRB with the ACIS-S/HETG instruments, and Piro et al.¹²⁾ reported the detection of both the iron emission line together with the Radiative Recombination edge and Continuum (RRC) from fully ionized iron with high statistical significance of 4.7σ and 3.0σ respectively. The redshift of the line and the RRC were consistent with the host galaxy, and the line was broadened to $\sigma_{\text{line}} = 0.23 \pm 0.07$ keV suggesting a moving ejecta of $0.05 c$. Soon after the Chandra detection, Antonelli et al.¹³⁾ also reported the probable iron emission line in the spectrum of GRB 000214 with $\sim 3.2 \sigma$ confidence level. This was the second detection of the iron with BeppoSAX. However the redshift of a host galaxy of GRB 000214 is unknown. Therefore, it remains a question whether the observed feature is the iron emission line or the RRC.

Motivated by the RRC detection with Chandra, Yoshida et al. 2000¹⁴⁾ apply the RRC for the ASCA data of GRB 970828 using the redshift of $z = 0.9578$, and obtain the edge energy, which is consistent with

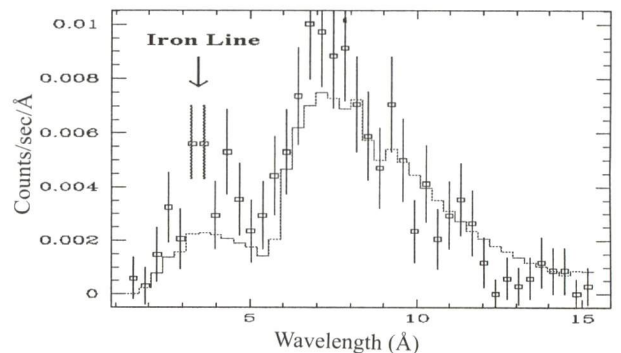


Fig. 3. The X-ray spectrum of GRB 991216 observed with the Chandra grating. A large excess at 3.5 \AA is clear with 4.7 sigma confidence level. The line is a little bit broadened than the instrumental resolution. The width corresponds to roughly $0.05 C$. The observed line energy permits only H-like iron.

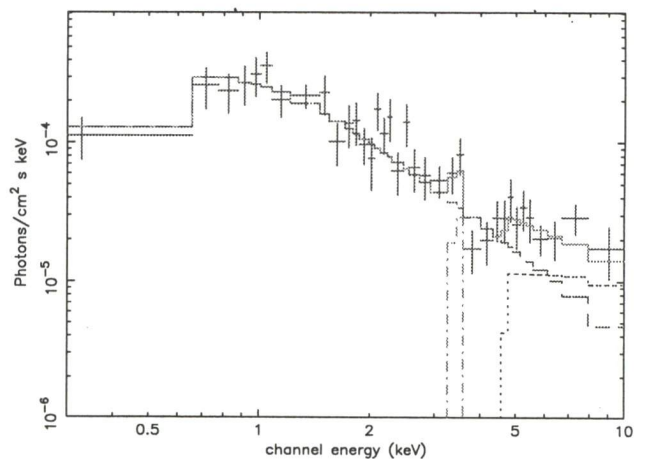


Fig. 4. The continuum spectrum with the ASIC detector on-board Chandra. The line emission is not so clear than the grating observation but the excess above the 4.4 keV over the continuum is clear. This can be interpreted as the result of the edge of Radiative Recombination edge and Continuum at 9.28 keV of H-like iron at the redshift of $z=1.00$ of the host galaxy.

9.28 keV. This possibility was earlier suggested in the paper by Djorgovski et al. (2001).¹¹⁾ The spectral feature matches to the 9.28 keV iron edge of the RRC but curiously there was no iron $K\alpha$ line detected at the expected energy from GRB 970828. The upper limit of the line flux is $< 1.5 \times 10^{-6}$ photons $\text{cm}^{-2} \text{s}^{-1}$ or 120 eV in equivalent width (EW). We must explain the no detection of $K\alpha$ line.

Thus, the existence of the strong iron features is now established by the later two observations but we should

note the fact that the iron features were found only in a small fraction ($< 10\%$) of X-ray afterglows, and sometimes the features were observed only during a certain interval (temporal). BeppoSAX has tried to search lines in eleven X-ray afterglow spectra, but found only one from GRB 970508 at the end of 1999 (Piro; private communication). Most X-ray afterglows did show only upper limits. Especially, Yonetoku et al.¹⁵⁾ set an extremely low upper limit of almost 100 eV in EW for the brightest GRB 990123 with ASCA. The most recent observation of GRB 010222 with Chandra suggests much lower upper limit of almost a few ten eV in EW (Yonetoku private communication). The published intensities of the observed iron $K\alpha$ line and the RRC are summarized in table I. There is a wide variety in the iron emission and the RRC intensity. In this paper, I try to explain these varieties of the iron features with the assumption that the line-emitting plasma state is in “non-equilibrium ionization (NEI) state” which has a low electron temperature as compared to the ionization degree. However I will not try to explain no iron line for most of them.

§3. Spectral Simulation for Non-equilibrium Plasma

To understand the physics of the iron line, we must first explain the variety of the observed iron feature. The observed flux of the RRC and the upper limit for the iron $K\alpha$ line are given for GRB 970828 with 90% confidence errors. So, we focus on the ratio of the integrated RRC flux to the iron intensity: $F_{\text{RRC}}/F_{\text{line}}$, which is free from the continuum. The line is much more simple than the continuum which consists mostly of non-thermal afterglow component. The observed ratio of: $F_{\text{RRC}}/F_{\text{line}} > 3.3$ in 90% statistical lower limit is very hard to reproduce. The case of a strong RRC without $K\alpha$ line looks abnormal. In fact, BeppoSAX detected the strong $K\alpha$ line and the Chandra observation showed both features of H-like iron with the flux ratio: $F_{\text{RRC}}/F_{\text{line}} \sim 1$. Therefore, we are forced to consider a different condition between ASCA and other results containing the strong $K\alpha$ line.

The no $K\alpha$ line of highly ionized iron accompanied by the recombination edge gives a constraint on the possible emission mechanisms. If the line were produced due to excitation by electron-impact, the RRC would be hidden by a much more intense thermal bremsstrahlung. Also the synchrotron emission, which is thought to dominate the afterglow, would be significantly overlaid by the thermal bremsstrahlung. Therefore, we need a condition that the iron is highly ionized but the involved electron energy is low. This is a radiative recombination in the NEI ($T_e < T_z$) state or charge exchange must be responsible for the iron emission.

In this section, we show spectra by numerical calculations in the NEI plasma state, not depending on the specific model. To explain the observed strong RRC without the $K\alpha$ line of iron, we calculate the emissivity using the NEI plasma radiation code by Masai 1994.¹⁶⁾ The code employs three mechanisms for the continuum, such as free-free emission, two-photon decay and radiative re-

combination. For line emissions, as well as excitation by electron-impact, fluorescence lines due to ionization and cascade lines due to recombination are taken into account but I do not discuss the detail of the code in this paper. Radiation properties of a plasma were described by two parameters of the electron temperature (T_e) and the ionization degree represented in units of temperature (T_z), assuming a cosmic abundance. We study the emissivities in the range of $0.1 < kT_e < 10$ keV and $0.1 < kT_z < 100$ keV in every 0.1 keV step.

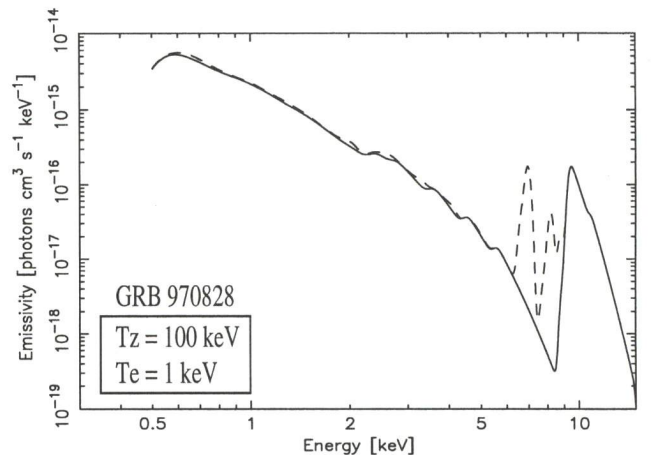


Fig. 5. Simulated emissivities, convolved with the energy resolution of the ASCA-SIS for the cases; $T_z = 100$ keV, $T_e = 1$ keV. The solid line represents emissivity of continuum and the dotted one is for emission lines. The figure is simulated for representing the cases of GRB 991216 and GRB970828 only in view point of the observed ratios of $F_{\text{RRC}}/F_{\text{line}}$. We do not intend to reproduce the spectral shapes, which mostly consist of a non-thermal component.

The strong RRC compared with the $K\alpha$ line can be formed only in the regime of $T_e < T_z$, recombining plasma condition. This condition is, however, attained by several situations as discussed later. We intend to find the condition of the plasma to account for the observed flux ratio ($F_{\text{RRC}}/F_{\text{line}}$), which is free from specific modeling with iron abundance, the emission measure, the geometry and so forth if the line and RRC are emitted from the same site. Thus, for a given T_e and T_z a priori, we carried out calculations of the emissivity ratio in the above wide range of $T_e - T_z$ space.

Figure 5 is the simulated plasma emissivities with a cosmic abundance to explain the ratio: $F_{\text{RRC}}/F_{\text{line}}$ of GRB 991216 and GRB 970828. In the calculation of the ratios, the line components (mostly the blend of Fe and Ni) very close to the edge of the RRC are included to the RRC component, due to the limited energy resolving power of the SIS detectors on-board ASCA.

§4. The Reason for Strong RRC and Weak $K\alpha$ Line

To produce the strong RRC in quantum number $n = 1$, the iron must be almost fully ionized. The H-like $K\alpha$ line,

Table I. Intensity of Iron Line and RRC

GRB Name	z	F_{line} (photons $\text{cm}^{-2}\text{s}^{-1}$)	σ (keV)	F_{RRC} (photons $\text{cm}^{-2}\text{s}^{-1}$)	kT (keV)	comments
970508 *	0.835	$(3.0 \pm 2.0) \times 10^{-5}$	—	—	—	* Piro et al. 1999, line intensity was variable
970828 †	0.958	$< 1.5 \times 10^{-6}$	—	$1.7^{+6.4}_{-1.2} \times 10^{-5}$	$0.8^{+1.0}_{-0.2}$	† Yoshida et al. 2001, RRC was temporal.
991216 ‡	1.020	$(3.2 \pm 0.8) \times 10^{-5}$	0.23 ± 0.07	3.8 ± 2.0	> 1.0	‡ Piro et al. 2000
000214 †	—	$(9 \pm 3) \times 10^{-6}$	—	—	—	† Antonelli et al. 2000
990123 *	1.600	$< 3.3 \times 10^{-6}$	—	—	—	* Yonetoku et al. 2000
990704 *	—	$< 4.7 \times 10^{-6}$	—	—	—	* Yonetoku et al. 2000

which was observed with Chandra, dominates other ionization states at a temperature of $kT_z > 20$ keV. Above the temperature, Fe XXVII consists of more than 70 % of iron, thus we assume $kT_z > 20$ keV in the following discussion. In a condition of high electron temperature of $kT_e \sim kT_z > 20$ keV, i.e., equilibrium ionization, the capture rate of free electrons is small and the emissivity of the line and RRC also becomes small. Moreover, the free-free emission from high T_e electrons dominates at the hard X-ray band. Therefore, the RRC may not be observed because it can be obscured by the free-free component.

The cross section of the electron capture into n th quantum state can be expressed as

$$\sigma_n \propto \frac{1}{n^3} \left(\frac{3kT_e}{2\epsilon} + \frac{1}{n^2} \right)^{-1} \quad (4.1)$$

where ϵ is an ionization energy of 9.28 keV for H-like iron.¹⁷⁾ Thus, the best condition to form the strong RRC would be the case of $kT_e \sim \epsilon$ ($\ll kT_z$). In such a plasma state, $\sigma_n \propto n^{-3}$ and then most of free electrons recombine directly into the ground state ($n = 1$), compared to the $n \geq 2$ levels. However, free-free emission dominates the continuum.

With decreasing kT_e , the recombination rate increases, while free-free emission becomes suppressed. Recombination into $n \geq 2$ increases relatively and produces line emission. Thus, the $K\alpha$ line can be enhanced by cascades from $n \geq 3$ excited levels. This is the case for He-like $K\alpha$, but H-like $K\alpha$ ($Ly\alpha$) is little affected; a considerable fraction comes to direct transition to the ground state.

We summarize the above discussions in view point of the intensity of the RRC and $K\alpha$ line. The plasma state with the strong RRC but the weak $K\alpha$ line, which was observed with ASCA, is realized when kT_e is slightly less than ϵ but in high kT_z . The peak of the ratio appears at around $kT_e = 4$ keV and $kT_z = 100$ keV in the calculated range. The condition of $F_{\text{RRC}}/F_{\text{line}} > 3.3$ of GRB 970828 can be explained by this result.

§5. Discussion

To explain the observed strong iron line and/or the RRC feature, a high ionization degree of $kT_z \sim 100$ keV and low electron temperature of $kT_e \sim 1$ keV are required when we reproduce the high ratio of the RRC to

the iron line more than 3.3 with a cosmic abundance. This condition may be attained in the situations: (i) photoionizations by X-rays or (ii) rapid cooling due to rarefaction.

In the case (i), also a fluorescence $K\alpha$ line of energies 6.4 – 6.5 keV of partially ionized iron is likely accompanied. Especially, the photoionizations of a neutral circumstellar gas by the initial bright flash of GRB, iron lines in the low ionization states are expected but not observed. The line observed with Chandra was purely H-like (Piro et al. 2000).¹²⁾ Therefore, the iron atoms should be fully ionized by the time of the observed iron emission. However, if the line and the RRC emitting region is illuminated continuously by a hidden intense beam, discussed by Rees et al. (2000),¹⁹⁾ it can achieve the NEI ($T_e < T_z$) state by the photoionization process. Even if this process works, the mean energy of the hidden-beam photons which illuminate the line emitting region should not be largely greater than the edge energy of 9.28 keV, since the observed values of T_e were low of $kT_e = 0.8^{+1.0}_{-0.2}$ keV at the rest frame for ASCA and $kT_e \sim 1$ keV for Chandra respectively.

We pay much attention to the case (ii) of a rapid adiabatic expansion of a highly ionized hot plasma. In this case, we are not required to assume abnormal iron abundance to explain the observed iron feature. This sort of mechanism to produce the strong iron Radiative Recombination edge and Continuum (RRC) with a cosmic abundance has already been investigated by Itoh & Masai¹⁸⁾ for a supernova which explodes in the circumstellar matter ejected during its progenitor's supergiant phase. They show that when the blast shock breaks out of the dense circumstellar matter into a low-density interstellar medium, a rarefaction wave propagates inward into the shocked hot plasma. Then the hot plasma expands adiabatically and loses its internal energy quickly. The electron temperature T_e decreases, but the ionization degree T_z temporally remains high, because the recombination time scale becomes much longer due to the low density. The temperature of the shocked matter, $kT \sim 100 (v_s/10^9 \text{ cm s}^{-1})^2$ keV where v_s is the shock velocity, drops by about two orders of magnitude for the density contrast (ratio) of the dense matter to the ambient medium of $\sim 10^3$ in their hydrodynamic cal-

culations. Therefore, the plasma can achieve the NEI ($T_e \sim 1 \text{ keV}$, $T_z \sim 100 \text{ keV}$) state naturally, and emit the strong RRC with the weak $K\alpha$ line of $F_{\text{RRC}}/F_{\text{line}} \sim 4$.

If these mechanisms work, we can estimate the required emission measure for GRB 970828 using the observed photon flux of the RRC (\mathcal{F}_{RRC}), the distance D and the integrated emissivity (ε_{RRC}) shown in the figure 5 with the cosmic abundance,

$$n^2 V \sim 10^{68} \left(\frac{D}{3 \text{ Gpc}}\right)^2 \left(\frac{\mathcal{F}_{\text{RRC}}}{1.7 \times 10^{-5}}\right) \left(\frac{\varepsilon_{\text{RRC}}}{2 \times 10^{-16}}\right)^{-1} \quad (5.1)$$

Although these n and V are coupled with each other and highly depend upon the specific model, we may conclude that the density of line emitting region is considerably high. If we adopt the size of 1 day light travel time in volume, the density of the mean ambient matter is 10^{10} cm^{-3} . This roughly corresponds to one solar mass of circumstellar matter with the cosmic abundance at the time of a supergiant phase of a massive star. This strongly suggests a massive star collapse forming a black-hole for a GRB.

Finally, one curious thing, which should be explained is that most of X-ray afterglow did not show both line and/or RRC feature, thus NEI is not always the case.

Acknowledgments

I would like to thank D. Yonetoku at ISAS and K.

Masai at Tokyo Metropolitan University for their assistances to write this report. This work was done under the support of Grant-in-Aides for the Scientific Research (Nos. 12640302) by the Ministry of Education, Culture, Sports, Science and Technology.

-
- 1) Kulkarni, S et al. : Nature **398** (1999) 389.
 - 2) Rees M. J. & Mészáros P.: MNRAS **258** (1992) L41.
 - 3) Piran T.: Phys. Rep. **314** (1998) 575.
 - 4) Dar A. & De Rújula A., : astro-ph/0008474 (2000) (A & A submitted)
 - 5) J.v.Paradijs, C. Kouveliotou and R.M.J.Wiljis: Ann. Rev. Astron. Astrophysics, **35** (2000).
 - 6) Paczyński B.: ApJ **494** (1998) L45
 - 7) Woosley S. E. : ApJ **405** (1993) 273.
 - 8) Vietri M. et al.: ApJ **507** (1998) L45.
 - 9) Piro L. et al.: ApJ **514** (1999) L73.
 - 10) Yoshida, A. et al.: A & A Sup. **138** (1999) 433.
 - 11) Djorgovski S. G. et al., : ApJ (submitted) (2001)
 - 12) Piro, L. et al.: Science **290** (2000) 955.
 - 13) Antnelli, L. A. et al.: ApJ, **545** (2000) L39.
 - 14) Yoshida et al.: ApJL, (2001) (submitted)
 - 15) Yonetoku, D. et al.: PASJ **52** (2000) 509.
 - 16) Masai, K., : ApJ **437** (1994) 770. 1
 - 17) Nakayama, M. & Masai, K.,: A & A (2001) Submitted
 - 18) Itoh, H. & Masai, K. : MNRAS **236** (1989) 885.
 - 19) Rees M. J. & Mészáros P. : ApJL **545** (2000) L73.
 - 20) Murakami, T. et al.: IAU Circ., (1997) # 6732